Royal College of Surgeons in Ireland



repository@rcsi.com

# Collagen scaffolds functionalised with copper-eluting bioactive glass reduce infection and enhance osteogenesis and angiogenesis both in vitro and in vivo.

AUTHOR(S)

Emily J. Ryan, Alan J. Ryan, Arlyng Gonzalez Vazquez, Anahí Philippart, Francesca E. Ciraldo, Christopher Hobbs, Valeria Nicolosi, Aldo R. Boccaccini, Cathal Kearney, Fergal J. O'Brien

## CITATION

Ryan, Emily J.; Ryan, Alan J.; Vazquez, Arlyng Gonzalez; Philippart, Anahí; Ciraldo, Francesca E.; Hobbs, Christopher; et al. (2019): Collagen scaffolds functionalised with copper-eluting bioactive glass reduce infection and enhance osteogenesis and angiogenesis both in vitro and in vivo.. Royal College of Surgeons in Ireland. Journal contribution. https://hdl.handle.net/10779/rcsi.10765331.v1

HANDLE

10779/rcsi.10765331.v1

LICENCE

## CC BY-NC-SA 4.0

This work is made available under the above open licence by RCSI and has been printed from https://repository.rcsi.com. For more information please contact repository@rcsi.com

URL

https://repository.rcsi.com/articles/journal\_contribution/Collagen\_scaffolds\_functionalised\_with\_coppereluting\_bioactive\_glass\_reduce\_infection\_and\_enhance\_osteogenesis\_and\_angiogenesis\_both\_in\_vitro\_and \_in\_vivo\_/10765331/1 Collagen scaffolds functionalised with copper-eluting bioactive glass reduce infection and enhance osteogenesis and angiogenesis both in vitro and in vivo

E.J. Ryan<sup>1,2,3</sup>, A.J. Ryan<sup>1,3,4</sup>, A. González-Vázquez<sup>1,3</sup>, A. Philippart<sup>5</sup>, F.E. Ciraldo<sup>5</sup>, C. Hobbs<sup>4,6,8</sup>, V. Nicolosi<sup>4,7,8</sup>, A.R. Boccaccini<sup>5</sup>, C.J. Kearney<sup>1,2,3,4</sup>, F.J. O'Brien<sup>1,3,4,\*</sup>

<sup>1</sup>Tissue Engineering Research Group (TERG), Dept. of Anatomy, Royal College of Surgeons in Ireland (RCSI), Dublin, Ireland, <sup>2</sup>Kearney Lab, Royal College of Surgeons in Ireland (RCSI), Dublin, Ireland, <sup>3</sup>Trinity Centre for BioEngineering (TCBE), Trinity College Dublin (TCD), Dublin, Ireland, <sup>4</sup>Advanced Materials and BioEngineering Research (AMBER), RCSI & TCD, Dublin, Ireland, <sup>5</sup>Institute of Biomaterials, University of Erlangen-Nuremberg, Germany, <sup>6</sup>School of Physics, TCD, Dublin, Ireland, <sup>7</sup>School of Chemistry, TCD, Dublin, Ireland <sup>8</sup>Centre for Research on Adaptive Nanostructures and Nanodevices (CRANN), TCD, Dublin, Ireland.

\* Corresponding author: Fergal J O'Brien,
Royal College of Surgeons in Ireland,
123 St. Stephens Green,
Dublin 2,
Dublin, Ireland.
Email address: fjobrien@rcsi.ie
Phone number: +353 1 402 2149

Running title: Copper-doped bioactive glass scaffold for osteomyelitis

#### Abstract

The bone infection osteomyelitis (typically by Staphylococcus aureus) usually requires a multistep procedure of surgical debridement, long-term systemic high-dose antibiotics, and - for larger defects - bone grafting. This, combined with the alarming rise in antibiotic resistance, necessitates development of alternative approaches. Herein, we describe a onestep treatment for osteomyelitis that combines local, controlled release of non-antibiotic antibacterials with a regenerative collagen-based scaffold. To maximise efficacy, we utilised bioactive glass, an established osteoconductive material with immense capacity for bone repair, as a delivery platform for copper ions (proven antibacterial, angiogenic, and osteogenic properties). Multifunctional collagen- copper-doped bioactive glass scaffolds (CuBG-CS) were fabricated with favourable microarchitectural and mechanical properties (up to 1.9-fold increase in compressive modulus over CS) within the ideal range for bone tissue engineering. Scaffolds demonstrated antibacterial activity against Staphylococcus aureus (up to 66% inhibition) whilst also enhancing osteogenesis (up to 3.6-fold increase in calcium deposition) and angiogenesis in vitro. Most significantly, when assessed in a chick embryo in vivo model, CuBG-CS not only demonstrated biocompatibility, but also a significant angiogenic and osteogenic response, consistent with in vitro studies. Collectively, these results indicate that the CuBG-CS developed here show potential as a one-step osteomyelitis treatment: reducing infection, whilst enhancing bone healing.

## Keywords

Osteomyelitis, copper, bioactive glass, antibacterial, osteogenesis, angiogenesis

#### 1. Introduction

Osteomyelitis is an infection localized to the skeletal system that is most commonly caused by the opportunistic gram-positive bacteria *Staphylococcus aureus* (*S. aureus*) and coagulase-negative staphylococci (~ 75% of cases combined) [1]. The clinical treatment of acute osteomyelitis usually involves 4-6 weeks of high-dose systemic antibiotic therapy. For chronic osteomyelitis, or in the case of a diffuse infection, substantial surgical debridement of the necrotic bone and surrounding soft tissue combined with high-dose systemic antibiotic therapy for up to 6 months is required [2]. Additionally, autologous bone grafting is often necessary to fill the void and support the defect site that remains after an aggressive debridement process [3,4].

Despite advances in the treatment of the disease through revised surgical approaches and antibiotic regimens [2,5], osteomyelitis remains notoriously difficult-to-treat with treatment failure rates of up to 20-30% [5,6]. As well as the drawback of the multistep treatment approach to osteomyelitis, the numerous complications associated with autografting for osteomyelitis (e.g. hematoma formation and donor site morbidity/fracture) are well documented [7]. Furthermore, the systemic administration of a sufficiently high dose of antibiotics to ensure that a therapeutic dose reaches the poorly vascularized, necrotic treatment site often results in systemic toxicity [8]. Therefore, in treating osteomyelitis, there exists a dual challenge: ensuring an effective and non-toxic dose of antimicrobial, while ensuring bone regeneration is stimulated.

Antibiotic resistance is now quickly becoming a serious risk to public health with more than 70% of hospital acquired bacterial infections being resistant to one or more of the antibiotics that were traditionally used to eradicate them [9]. In parallel, there has been a steep decline in antibiotic approval over the last 30 years, with only five antibiotics approved by the US Food and Drug Administration (FDA) between 2012 and 2017 [10]. Minimal new antibiotic approvals combined with an alarming number of emerging cases of microbial resistance to 'last resort' antibiotics (e.g. vancomycin) motivate the requirement for non-antibiotic alternatives, such as ionic metals (e.g., copper, silver).

Copper is a well-known antimicrobial material that can also contribute to bone generation through stimulation of osteogenesis and angiogenesis. Copper has been shown to be effective against both gram-positive and gram-negative bacteria and fungi [11–13]. Furthermore, copper ions can enhance bone formation by maturation of collagen through lysyl oxidase crosslinking [14] and by inducing osteogenic differentiation of mesenchymal

3

stem cells (MSCs) [15]. The effect of copper on vascular stimulation results from its ability to stimulate bone marrow derived stem cells to produce vascular endothelial growth factor (VEGF); VEGF induces vascularization, which is essential for successful tissue regeneration [16,17]. Despite the promise of antimicrobial materials in the field of regenerative medicine, there is a trade-off between bacteria-killing ability and inducing toxic effects to healthy cells in the body and, therefore the dosage level of copper is critical. One strategy to control the dosing of copper is to deliver it locally at the defect site using a carrier material that modulates its release profile.

Tissue engineered scaffolds that mimic the natural extracellular matrix can provide a template for tissue repair by providing structural support for cells in a 3D environment. In our lab, we have previously developed a series of highly porous collagen-based scaffolds for a variety of tissue regeneration applications [18–22]. Collagen is natural, biodegradable, facilitates cell attachment and migration, and does not elicit a host immune response [23]. In bone, it makes up 89% of the organic matrix and 32% of the volumetric composition [23]; however, collagen scaffolds typically have poor compressive strength in comparison to native bone. Therefore, for use as scaffolds for bone tissue engineering, it is advantageous to combine collagen with another material for structural integrity. By careful selection of the secondary material, additional advantages can be added to the collagen scaffold system (e.g., osteogenic ceramics like hydroxyapatite [24] or bioactive glass).

For this reason, we have utilised copper-doped bioactive glass (CuBG) as a non-antibiotic antibacterial that can stimulate bone regeneration, which we hypothesised might also enhance the stiffness of a collagen scaffold. Bioactive glass is an osteoinductive, biocompatible, and biodegradable material that was first developed by Larry Hench and colleagues in 1969 [25]. Bioactive glass is usually fabricated from a combination of calcium, phosphorous, silica, and sodium. Upon implantation, a layer of hydroxyapatite forms on the surface of BG that can develop firm bonds with bone and soft tissue [17,25]. Following this, growth factors are thought to readily bind to the apatite layer and cellular attachment ensues. Osteoprogenitor cells are then differentiated into osteoblastic cells due to the hydroxyapatite stimulus and result in bone formation. BonAlive (BAG-S53P4) is a commercial bioactive glass product currently being used to treat osteomyelitis, whose antibacterial activity is attributed solely to local pH and osmotic pressure changes [26]. However, other elements can be substituted into the silica network for enhanced bioactivity including stimulation of angiogenesis (e.g. cobalt),[27] bone formation (e.g. zinc) [28], and, most importantly in this application, antimicrobial activity (copper) [16,17,29]. Thus, the

4

combination of copper and bioactive glass might act as a multifunctional material that is antibacterial, osteoinductive, and angiogenic [16,17].

We thus hypothesised that combining copper-doped bioactive glass with a porous 3D collagen scaffolds (CuBG-CS) with proven regenerative capacity [19,27,30–32] would result in an off-the-shelf scaffold for osteomyelitis treatment that elicits osteo- and angiogenesis, whilst, most importantly, limiting infection. We first explored the dose-response of copper ions alone on bacterial toxicity and mammalian cell viability in 2D culture to determine appropriate concentrations for incorporation into the scaffolds. Next, we developed a method for incorporating varying concentrations of CuBG into the collagen scaffold and investigated the effect of CuBG addition on scaffold mechanical and microarchitectural properties. The copper ion release and antibacterial activity of the CuBG-CS was then explored before assessment of the ability of the scaffolds to support osteogenesis and angiogenesis in vitro. Finally, we assessed the osteogenic and angiogenic response of the bioactive glass scaffolds in a chick embryo ex ovo model.

#### 2. Materials and methods

All materials used were purchased from Sigma Aldrich Ireland, unless otherwise stated.

#### 2.1 Effect of copper ions on bacterial toxicity and mammalian cell viability in 2D culture

To identify an appropriate concentration range of copper-doped bioactive glass to incorporate into the collagen scaffold, the effect of copper ions on bacterial and mammalian cells in 2D culture was first assessed. A range of copper chloride concentrations (equivalent to  $0 - 1.02 \text{ mg Cu}^{2+}/\text{ml}$ ) was added to 100 µl of Brain Heart Infusion (BHI) broth in a 96-well plate (n=3 per group). *Staphylococcus aureus* (*S. aureus*) Newman was added to the wells at 5x105 Colony Forming Units (CFU)/ml and the plate was incubated at 37°C for 24 hours. The optical density or opacity of the solutions was measured using a spectrophotometer. The minimum inhibitory concentration (MIC) of copper chloride was considered to be the lowest concentration at which no visible bacterial growth occurred according to spectrophotometric readings. To find the minimum bactericidal concentration (MBC) of copper chloride, 10 µl of the solutions from the remaining visually clear wells were added to BHI agar plates, allowed to air dry for 15 minutes, and then incubated for 24 hours at 37°C. The lowest concentration on the solutions that did not show any growth was termed the MBC.

A pre-osteoblast cell line (MC3T3-E1, ECACC, UK) were seeded in 96-well plates at 10,000 cells/well in 100 µl of medium containing the same range of copper chloride concentrations (equivalent to 0 – 1.02 mg Cu<sup>2+</sup>/ml) (n=3 per group) and the cells were incubated under standard culture conditions (37°C, 5% C02, and 95% relative humidity) for 24 hours. The cells were washed 2X with phosphate buffered saline (PBS) and lysed (100 µl of 0.2 M sodium carbonate with 1% Triton). The resulting lysate was analysed for DNA content as an indicator of cell number using a Quant-iT<sup>™</sup> PicoGreen<sup>™</sup> dsDNA Assay Kit (Molecular Probes, USA) as per the manufacturer's instructions.

#### 2.2 Bioactive glass synthesis and characterisation

Bioactive glass with and without a maximum achievable concentration of 2% (mol) copper (equivalent to 0.02 mg Cu<sup>2+</sup>/mg BG) was prepared by a sol-gel process. The composition of the bioactive glasses is as follows:

	BG (mol%)	CuBG (mol%)
Silicon dioxide (SiO <sub>2</sub> )	60	60
Calcium oxide (CaO)	36	34
Phosphorus pentoxide (P <sub>2</sub> O <sub>5</sub> )	4	4
Copper oxide (CuO)	0	2

Table 1 Composition (Mol%) of sol-gel derived 0% and 2% copper-doped bioactive glass

#### Particle size

The bioactive glass was ground and sieved to obtain particles of less than 100  $\mu$ m in size - a size previously deemed suitable by our group for both osteogenesis and a reduced immune response [33,34]. The resulting bioactive glass particles were sized by dynamic light scattering using a Mastersizer 2000 (Malvern Instruments, UK). Briefly, 5 mg of bioactive glass was suspended in 5 ml of 100% ethanol and was added dropwise to the dispersant chamber containing ethanol under stirring at 1260 rpm until the laser obscuration value was approximately 10%. Particle size was measured and repeated in triplicate. The refractive index of the ethanol and bioactive glass were taken to be 1.36 and 1.545, respectively [35,36].

#### XRD analysis

X-ray diffraction analysis was carried out using a Rigaku Miniflex X-ray diffractometer with a 2Theta range from 10° to 80° and a step size of 0.02°. Cu K $\alpha$  radiation was used for the measurement.

#### 2.3 Collagen - bioactive glass composite scaffold fabrication

Having identified the optimal concentration range of copper required to kill bacteria and minimise mammalian cell toxicity, we estimated the appropriate concentration range of 2% (mol) copper-doped bioactive glass to incorporate into the collagen scaffolds (300% CuBG = 0.3 mg Cu<sup>2+</sup>/ml). The scaffolds were fabricated by freeze-drying a co-suspension of collagen and bioactive glass particles (+/- copper doping, referred to as CuBG and BG, respectively) at a range of different concentrations (collagen only, 20%, 100%, and 300% BG or CuBG w/w bioactive glass to collagen), similar to methods previously developed within our group to

incorporate ceramics into collagen scaffolds [27,34,37]. Briefly, a collagen slurry was produced by mixing type I collagen (5 mg/ml) isolated from bovine tendon in aqueous 0.5 M acetic acid solution (Fisher Scientific, UK). Bioactive glass was added to the collagen slurry and was mixed between two syringes connected with a luer lock until a homogeneous suspension was obtained. The slurry suspension was then degassed using a vacuum chamber and freeze-dried in a custom built mould (10 mm  $\emptyset$  x 5mm discs) until a final temperature of -40°C using a previously optimised freeze-drying profile [38]. Scaffolds were sterilised and physically crosslinked using dehydrothermal (DHT) treatment at 105°C for 24 hours at 0.05 bar [39]. Scaffolds were then further chemically crosslinked using EDAC [1-ethyl-3-(3-dimethyl aminopropyl) carbodiimide] (6 mM) and NHS (N-hydroxysuccinimide) (2.4 mM) in distilled water for two hours, followed by 2X washes in PBS [40].

#### 2.4 Physical characterisation of collagen-bioactive glass scaffolds

# Distribution of bioactive glass within scaffold & effect of bioactive glass addition on scaffold porosity and pore size

Scanning electron microscopy (SEM) was used to characterize the scaffold morphology, porosity, and bioactive glass distribution. Scaffold samples were prepared for SEM analysis by mounting onto SEM stubs and imaged using a Carl Zeiss Ultra SEM equipped with a secondary electron detector and energy selective backscatter detector (Carl Zeiss, Germany). The porosity of the bioactive glass scaffolds was calculated by measuring the density of the scaffold in relation to the density of the individual scaffold components as per (Equation 1, below.

Scaffold porosity (%) = 
$$\left(1 - \frac{\rho_{\text{scaffold}}}{(\rho_{\text{collagen}})(\% \text{ wt collagen}) + (\rho_{\text{bioactive glass}})(\% \text{ wt bioactive glass})}\right)$$
 (Equation 1)

The scaffold density was calculated by dividing the measured weight (Digital scale, Mettler Toledo MX5; Mason Technology, Dublin, Accuracy 0.01 mg) by the volume, using an average of two diameter and height measurements per scaffold (Vernier callipers, Krunstoffwerke; Radionics, Dublin, Ireland). The theoretical density of collagen and bioactive glass used were 1.3 and 2.7, respectively [41,42]. For scaffold pore size analysis, scaffolds were sectioned longitudinally and SEM images of all scaffolds were captured at 150X. The mean pore diameter was analysed using Image J. Briefly, for each pore selected at random, the maximum diameter and the diameter perpendicular to the maximum were averaged and the mean pore diameter calculated from these values (n=30 pores per group).

#### Effect of bioactive glass addition on scaffold mechanical properties

In order to investigate the effect of bioactive glass addition on scaffold compressive modulus, unconfined, wet compression testing of the scaffolds was performed using a uniaxial tensile testing machine (Z050, Zwick/Roell, Germany) fitted with a 5 N load cell [39]. Scaffolds were pre-hydrated in PBS and tested at a rate of 10% strain/minute up to a maximum strain of 10%. The compressive modulus of the scaffolds was calculated in the 2-5% strain range (n=5 scaffolds, 3 repeats per scaffold).

#### 2.5 Antibacterial characterisation of bioactive glass scaffolds

#### Cu<sup>2+</sup> ion release from bioactive glass scaffolds

Scaffolds (n=3) were incubated in 1 ml deionised water at 37°C. The eluate was collected at days 1, 3, and 7. The copper ion content was measured using a Copper Assay Kit. All samples and standards were run in triplicate.

#### Antibacterial activity in broth up to 7 days

In order to assess antibacterial activity, the scaffolds were added to Brain Heart Infusion (BHI) broth (n=3) and incubated at 37°C. At day 1, 3, and 7 scaffolds were removed and  $5\times10^5$  CFU/ml of *S. aureus* were added to the eluate. The solutions were incubated for a further 24 hours and the percentage bacterial growth was quantified as described above. Positive and negative bacterial growth controls (+/- *S. aureus*) were used.

#### <u>Time-kill assay</u>

A time-kill assay was performed to determine the effect of the scaffolds on the growth rate of *S. aureus*. Scaffolds were added to 1 ml Brain Heart Infusion (BHI) broth (n=3) in 24-well plates and 5x105 CFU/ml of *S. aureus* Newman were added. The plates were incubated in a shaker (150 rpm, 37°C) and the optical density was measured (with scaffolds temporarily removed) using a plate reader every hour over 24 hours.

#### 2.6 Biological characterisation of bioactive glass scaffolds - Analysis of osteogenesis

#### Cell culture and seeding

To assess the ability of the bioactive glass scaffolds to support osteogenesis, MC3T3-E1 cells were cultured in growth medium consisting of Alpha Minimum Essential Medium ( $\alpha$ -MEM) supplemented with 10% Foetal Bovine Serum (FBS) (Labtech, UK), 2% penicillin/streptomycin, and 1% L-Glutamine. All scaffolds were seeded with 500,000 cells

and were cultured in growth medium for the first two days prior to supplementation with osteogenic medium. For MC3T3-E1 osteogenic medium, the following supplements were added to the above described growth medium: 50  $\mu$ M ascorbic acid 2-P, 100 nM dexamethasone, and 10 mM  $\beta$ -glycerophosphate. All cells were cultured under standard culture conditions (37°C, 5% C02, and 95% relative humidity).

#### DNA quantification

DNA, as an indicator of cell number and survival, was quantified using a Quant-iT<sup>™</sup> PicoGreen<sup>™</sup> dsDNA Assay Kit (Molecular Probes, USA). Three scaffolds per group (n=3) at each time point (days 0, 7, 14, and 28) were washed twice in PBS, added to 1 ml lysis buffer (0.2 M carbonate buffer with 1% Triton), and the scaffold solutions were subjected to three freeze-thaw cycles at -80°C to assist in cell lysis. The resulting lysate was analysed for DNA content as per the manufacturer's instructions. The background reading obtained from cellfree control scaffolds cultured under identical conditions to the test samples was subtracted from cell-seeded sample readings.

#### Cell-mediated mineralisation

Cell-mediated calcium production was quantified using a Calcium (CPC) LiquiColor<sup>TM</sup> test (Stanbio, Ireland). Three scaffolds per group (n=3) at day 14 and 28 were added to 1 ml of 0.5 M hydrochloric acid. Samples were left shaking overnight at 4°C before performing the assay as per the manufacturer's instructions. As the bioactive glass samples inherently contain calcium, the background reading – obtained from cell-free control scaffolds cultured under identical conditions to the test samples – was subtracted from the sample readings. Alizarin red staining was performed to assess the distribution of cell-mediated calcium distribution. Briefly, scaffolds were fixed in 10% paraformaldehyde, embedded in paraffin wax, and sectioned using a microtome (Leica RM 2255, Leica, Germany) to 5  $\mu$ m thick slices. Sections were placed on glass slides, de-paraffinised to distilled water, stained using 2% alizarin red solution for 2 mins, washed with deionised water, and mounted with DPX solution before adding a coverslip. Sections were imaged using a digital microscope (Nikon Eclipse 90i, Nikon Instruments Europe).

#### 2.7 Biological characterisation of bioactive glass scaffolds - Analysis of angiogenesis

#### Cell culture and seeding

Angiogenesis was assessed using Human Umbilical Vein Endothelial Cells (HUVECs) and Rat Mesenchymal Stem cells (rMSCs). HUVECs were cultured in EndoGRO complete culture

medium (SCME002, Merck Millipore) and rMSCs were cultured in high-glucose DMEM (D5671) medium supplemented with 10% FBS, 2% penicillin/streptomycin, 1% Glutamax, and 1% Non-Essential Amino Acids (Biosciences, Ireland) and 1% L-Glutamine. All cells were cultured under standard culture conditions (37°C, 5% C02, and 95% relative humidity).

#### Matrigel assay

The ability of the eluate from the copper-doped bioactive glass scaffolds to support tubule formation was assessed using a Matrigel<sup>®</sup> assay. Cell-free scaffolds (n=3) were placed in 1 ml of endothelial medium and incubated at 37°C under standard cell culture conditions. The eluate from the scaffolds was collected at day 1, 3, and 7 and stored at -80°C until use. Matrigel<sup>®</sup> basement membrane matrix (Corning, USA) was added to 24-well plates (120 µl/well) and the plates were incubated for 30 mins at 37°C. HUVECs were seeded at 30,000 cells/well and 1 ml of the medium eluate was added. At 36 hours the Matrigel cultures were imaged using a digital microscope (Leica DMIL, Leica microsystems). Three images per well were captured at 10X magnification and images were analysed for total tubule length using ImageJ software and an in-house developed plug-in.

#### VEGF protein production

Cell-free scaffolds (n=3) were placed in 2ml of cell culture medium and incubated at 37°C under standard cell culture conditions. rMSCs were seeded in 6-well plates (n=3) at a density of 50,000 cells/well. 2 ml of eluate from the scaffolds was collected at day 1, 3, and 5 and added directly to the rMSCs. At day 7 the cell culture medium was harvested and analysed for VEGF protein production using ELISA (R&D Systems, USA). 1 ml of lysis buffer was then added to the wells and DNA was quantified as previously described. A cell-only control using regular rMSC growth medium was used.

# 2.8 Analysis of copper-doped bioactive glass scaffolds on osteo- and angiogenesis in a chick embryo ex ovo model

Here, we utilise an established in vivo model – the ex ovo or shell-less chicken embryo model – to further demonstrate the therapeutic effect of the bioactive glass scaffolds previously tested in vitro [43–46]. The chicken ex ovo embryo model allows us to examine the effect of the scaffolds on both angiogenesis and osteogenesis. The angiogenic effect of therapeutics applied to the ex ovo chicken embryo can be visually examined on the highly vascularised chicken chorioallantoic membrane (CAM) which surrounds the embryo. During development, like humans, the limbs of chicken embryos undergo endochondral ossification

and thus by culturing the chicken embryos up to a maximum of 12 days of development (whilst the limbs remain mainly cartilaginous), the osteogenic effect of therapeutics can be examined by looking for accelerated endochondral ossification.

Fertilised chicken eggs (day 0 of development) were supplied by Ovagen (Ovagen Group Ltd, Co. Mayo, Ireland). On receipt, the eggs were incubated for 3 days (until day 3 of development) lying in a horizontal position in a cell-culture incubator at 37°C in regular atmospheric gas. The eggs were turned every 24 hours for correct embryo orientation during development and for optimum CAM development [47]. On day 3, the eggs were cracked into 100 mm Ø petri dishes (Corning Inc., New York, USA) and the lid was replaced. To keep the embryos humidified, the petri dish containing the embryo was placed into a larger 150 mm  $\emptyset$  petri dish (Corning Inc., New York, USA) containing 25 ml of sterile PBS and the lid of the larger petri dish was also replaced and the chick embryos were placed back in the incubator. After a further 4 days of incubation (until day 7 of development), the BG-CS and CuBG-CS were placed on the CAM membrane (6 mm Ø scaffolds hydrated in PBS). As controls, collagen only scaffolds soaked in either PBS, 1 μg of recombinant VEGF (Vascular Endothelial Growth Factor) or 1.5 µg of recombinant BMP-2 (Bone Morphogenic Protein-2) (PeproTech, United Kingdom) were placed on the embryos. The chick embryos were then incubated for a final 5 days (until day 12 of development) and the effect of the scaffolds on both angiogenesis and osteogenesis was analysed, as described below.

All experimentation carried out on chick embryos was in accordance with the EU Directive 2010/63/EU for animal experiments.

#### Osteogenesis studies

After analysing angiogenesis, the embryos were culled using formalin solution and embryo death was confirmed by decapitation. The hind limbs of the embryos were dissected and transferred to fresh 10% formalin solution overnight. Next, the hind limbs of the chick embryos were differentially stained for cartilage and bone following a protocol by Wassersug et al. [48]. Briefly, the excess skin and tissue surrounding the femur and tibia/fibula were removed carefully and the specimens were washed in a series deionised water changes. The limbs were then placed in an alcian blue staining solution (9 mg alcian blue 8GX, 60 ml absolute ethanol, 40 ml glacial acetic acid) for 24 hours. Next, the limbs were dehydrated in absolute ethanol for 24 hours. After dehydration, the limbs were placed in 0.5% potassium hydroxide (KOH) solution with 3 or 4 drops of 0.1% alizarin red S solution to every 100 ml of KOH solution for 24 hours. Finally, the limbs were cleared by transferring specimens to 100%

glycerol through a series of glycerol-water solutions – 25%, 50%, 75%, and 100%. The limbs were imaged for signs of accelerated osteogenesis (alizarin red staining) using a stereo microscope at 10X magnification (Leica Microsystems, Germany).

#### Angiogenesis studies - blood vessel quantification

The local effect of the scaffolds on angiogenesis of the CAM was analysed by quantifying the blood vessel density in the region surrounding to the scaffold. On day 12, the scaffolds and surrounding CAM of all chick embryos were imaged. The images were analysed for blood vessel density by developing a novel method using Fiji software (ImageJ) (**Figure 1**). Briefly, images were scaled and cropped appropriately and the 'Mexican Hat Filter' plugin was applied (radius 5.0). Next, images were converted to 8-bit and the threshold was adjusted to a set level where all blood vessels were highlighted appropriately (lower threshold: 0, upper threshold: 150). Finally, a 12.5 mm  $\emptyset$  circle was drawn centred around the scaffold and the percentage of that area that contained blood vessels was quantified using the measure tool (n=3 embryos analysed for each treatment group).

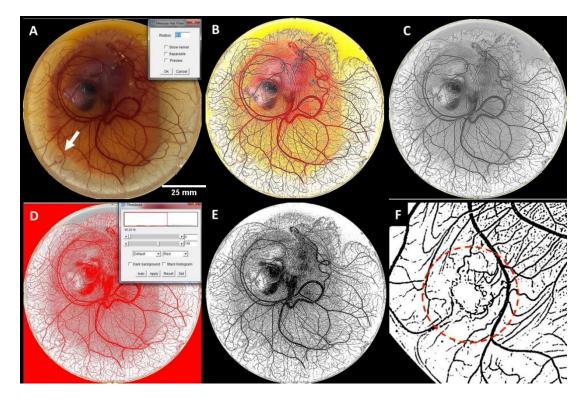


# Figure 1 Method used to analyse effect of the scaffolds on angiogenesis in a chick CAM membrane using Fiji software (ImageJ)

(A) Scaled and cropped image of whole CAM membrane containing scaffold (indicated by the white arrow). (B) Image after 'Mexican Hat Filter' plugin was applied. (C) Image converted to 8-bit. (D) Thresholding of image to include all blood vessels. (E) Image after threshold was applied. (F) Region around scaffold where the percentage blood vessel area was measured.

#### 2.9 Statistical analysis

Data are presented as mean +/- standard deviation. Statistical analysis was performed using GraphPad Prism software. Two-tailed unpaired t-tests or one-way or two-way ANOVAs were conducted where appropriate followed by a Bonferroni post-hoc test for multiple pairwise comparisons between groups. A P-value of 0.05 or less was considered statistically significant ( $p \le 0.05$ ). The Pearson product correlation coefficient (r) was used to determine the strength and direction of a linear relationship. An r value of 0.7-1 was considered a strong positive correlation. Three biological and three technical repeats were performed for all experiments and assays.

#### 3. Results

# 3.1 Copper ions effectively eliminate *Staphylococcus* aurovith viable mammalian cells remaining

A range of copper chloride concentrations were utilised to determine the effect of  $Cu^{2+}$  exposure on both bacterial and mammalian cells in 2D culture. Increasing copper ion concentration decreased cellular viability of both *S. aureus* and osteoblasts after 24 hours (**Figure 2**). Both the minimum inhibitory concentration (MIC) and minimum bactericidal concentration (MBC) of  $Cu^{2+}$  against *S. aureus* Newman was found to be 1.02 mg/ml. While a reduction in mammalian cell viability was observed at concentrations above 0.06 mg  $Cu^{2+}/ml$ , increasing the copper concentration further did not have any additional effect on mammalian cell viability. By contrast, concentrations of copper chloride above 0.51 mg  $Cu^{2+}/ml$  almost completely eliminated *S. aureus* growth (MIC/MBC concentrations).

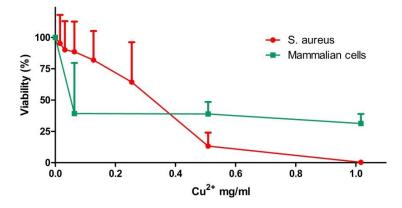


**Figure 2 Effect of copper chloride on** *S. aureu***and pre-osteoblast cells (MC3T3-E1)** The viability of pre-osteoblast cells or *S. aureus* cultured with increasing concentrations of copper chloride was analysed using DNA quantification and spectrophotometric growth quantification, respectively. Note: Viability of mammalian cells is normalized to cells seeded into the well plate with 0 mg/ml copper chloride (regular growth media) and viability of *S. aureus* is normalized to bacteria with 0 mg/ml copper chloride (regular BHI growth broth).

These results highlight the fine balance between bacteria-killing ability and toxic effects towards mammalian cells, emphasising the need to control the dosage level to achieve a suitable bacteria killing/mammalian cell survival ratio. This motivates the application of local and controlled release of copper ions while providing some basis for requisite dosing for the proposed biomaterial system.

#### 3.2 Characterisation of copper-doped bioactive glass

Bioactive glass (with and without copper) was fabricated via a sol-gel method, ground, and sieved. The resulting particles ranged between 2-100  $\mu$ m, as per dynamic light scattering

(Figure 3A). XRD showed that the incorporation of Cu generated copper oxide (CuO), and peaks at  $2\theta = 35^{\circ}$ ,  $40^{\circ}$  and  $47^{\circ}$  were developed (Figure 3B). The presence of CuO crystals in these systems likely depends on the conditions used during the sol–gel process and the amount of copper added. These results are in agreement with those obtained by Bejarano *et al.* [49].

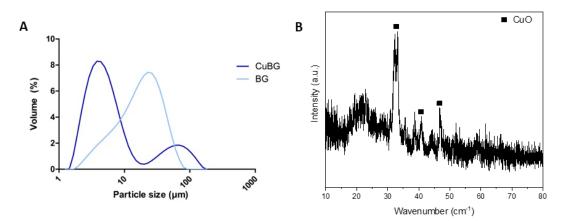


Figure 3 Characterisation of copper-doped bioactive glass particles (A) The size range of bioactive glass particles (2-110  $\mu$ m). (B) X-ray diffraction (XRD) spectrum of copper-doped bioactive glass.

# 3.3 Bioactive glass addition resulted in highly porous scaffolds with suitable pore size and increased compressive modulus

Having determined the effect of copper ions alone on osteoblasts and S. aureus in 2D, we next incorporated the copper into bioactive glass, utilising it as a local delivery vehicle within a collagen scaffold. It was found that 300% CuBG was the maximum concentration of bioactive glass that could be incorporated into the scaffold as a higher concentration of bioactive glass caused the pH of the slurry to change, causing it to separate. Scanning electron microscope (SEM) images revealed the highly porous, interconnected, open structure of the copper-doped bioactive glass scaffold even at the highest achievable concentration (300% CuBG) (Figure 4A). Energy selective backscatter SEM (BSEM) images showed a homogenous distribution of copper-doped bioactive glass in the collagen scaffold, demonstrated by the bright particles dispersed throughout the darker scaffold materials (Figure 4B). This material contrast is due to the relatively higher atomic number of the copper-doped particles, i.e. Z-contrast. There was a significant, albeit marginal, change in scaffold porosity upon bioactive glass addition; however, even upon the incorporation of 300% CuBG, all scaffolds remain extremely porous at more than 98%, which is greater than the reported suitable porosity required for tissue engineering applications (90%) (Figure 4C) [50]. The addition of bioactive glass did not significantly affect scaffold pore size, with all

scaffolds achieving a mean pore size ranging from 68-79  $\mu$ m (**Figure 4**D), a suitable size for osteogenesis and angiogenesis in collagen-based scaffolds [51–53]. Notably, increasing bioactive glass concentration increased scaffold compressive modulus with a linearly increasing trend (r = 0.9991), with the 100% CuBG-CS increasing compressive modulus by 1.6-fold and 300% CuBG-CS significantly increasing compressive modulus (p < 0.05) by 2.7-fold versus the collagen control (**Figure 4**E).

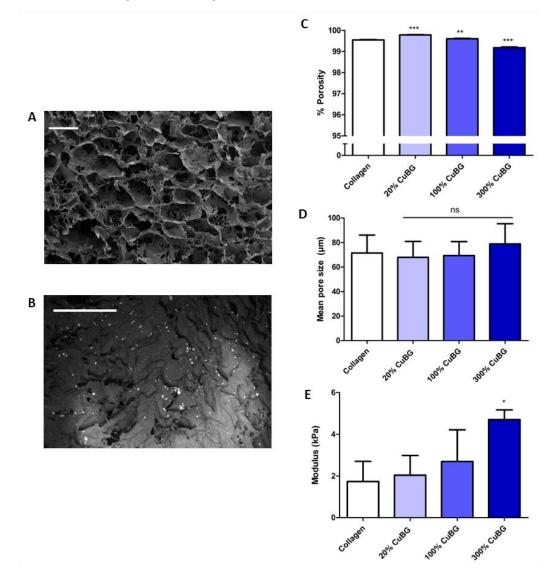


Figure 4 Effect of bioactive glass addition on scaffold microarchitectural and mechanical properties (A) SEM image showing the highly porous open structure of scaffold containing the highest concentration of bioactive glass (300% CuBG). (B) Energy-selective backscatter SEM image showing homogeneously distributed bioactive glass. Note: material contrast images highlighting bright copperdoped particles compared to the darker collagen background. (C) All scaffolds remain highly porous (>98%) upon incorporation of copper-doped bioactive glass. (D) Copper-doped bioactive glass addition does not significantly alter scaffold pore size in comparison to the collagen control. (E) Increasing copper-doped bioactive glass addition increases scaffold compressive modulus with a linear trend, with 300% CuBG-CS having a significantly higher compressive modulus than the collagen control. Note: scale bars 100  $\mu$ m. Data presented as mean ± SD, n=3, p-values are calculated using one-way ANOVA with Bonferroni post-hoc test, all statistical significance shown in comparison to collagen control unless otherwise stated, \*p < 0.05, \*\*p < 0.01, \*\*\*p < 0.001.

Having determined that collagen scaffolds functionalised with copper-doped bioactive glass remain highly porous and show increased mechanical properties, we next sought to determine the scaffold's principal function – its antibacterial activity against *S. aureus*.

# 3.4Copper-doped bioactive glass scaffolds reduce the viability of *Staphylococcus* aureus

Of the concentrations tested, 300% CuBG scaffolds released the highest dose of copper ions within 24 hours (**Figure 5**A) which resulted in a significantly increased antibacterial activity versus all other groups, inhibiting *S. aureus* growth by up to 66% (**Figure 5**B) (p < 0.01 & p < 0.001). A time-kill assay shows that 100% CuBG-CS also significantly delayed the growth of *S. aureus* at 7 hours (p < 0.05) and 300% CuBG-CS significantly delayed the growth of *S. aureus* from 7 to 24 hours (p < 0.001) in comparison to the collagen control (**Figure 5**C).

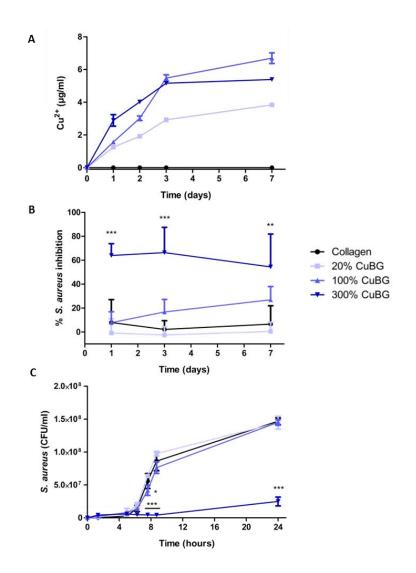


Figure 5 Effect of bioactive glass addition on scaffold antibacterial activity

(A) Copper ion release from copper-doped bioactive glass scaffolds over 7 days. (B) Effect of incorporation of copper-doped bioactive glass in collagen scaffolds on the inhibition of *S. aureus* Newman growth after 1, 3, and 7 days (normalized to regular BHI growth broth without scaffold inoculated with *S. aureus*). (C) Time-kill graph for copper-doped bioactive glass scaffolds. Data presented as mean  $\pm$  SD, n=3, p-values are calculated using one-way ANOVA with Bonferroni post-hoc test, all statistical significance shown in comparison to collagen control unless otherwise stated, \*p < 0.05, \*\*p < 0.01, \*\*\*p < 0.001.

These analyses demonstrate the desired antibacterial effect of the 100% and 300% CuBG-CS. Therefore, the osteogenic and angiogenic potential of the 100% and 300% CuBG-CS (and 100% and 300% BG-CS controls, i.e., non-copper doped) was next examined. The 20% CuBG-CS was discontinued from further studies from here on due to its lack of antibacterial properties.

#### 3.5 Copper-doped bioactive glass scaffolds enhance osteogenesis in vitro

Having demonstrated the antibacterial potential of the CuBG-CS, we next tested the scaffold's ability to maintain mammalian cell viability and promote osteogenesis. This is crucial given the fine balance between antibacterial activity and mammalian cell toxicity as identified above (Figure 2). The results show that 300% CuBG-CS significantly increased cell proliferation after initial seeding in growth medium at 72 hours (p < 0.05), by 1.5-fold in comparison to the collagen control (Figure 6A). This was a positive result as, based on its pronounced antibacterial properties, we had some concern that incorporating levels as high as 300% CuBG in the scaffolds might reduce mammalian cell viability; furthermore, although some reduction was seen in cell number at later time points in osteogenic medium (Day 7 and beyond) for the 300% CuBG-CS, it was not significantly different in comparison to collagen controls at any time point (Figure 6B). With the exception of the 300% CuBG-CS, there is an increase in cell number on all scaffolds containing bioactive glass (either BG or CuBG) (Figure 6B). With regards to osteogenesis, the 300% CuBG-CS demonstrated significantly increased cell-mediated calcium deposition at days 14 and 28 vs the 300% BG-CS controls (p < 0.001 for all) (Figure 6C). The osteogenic capacity of CuBG-CS was confirmed with alizarin red staining, which showed increased calcium deposition that was homogeneously distributed throughout the scaffold cross-section (Figure 6D). By contrast, the less mechanically robust collagen-only control showed an encapsulation effect, where mineralisation only occurred on the scaffold periphery. Taken together, these results demonstrate that the 300% CuBG-CS not only support osteogenesis but enhances it in comparison to the other scaffold groups.

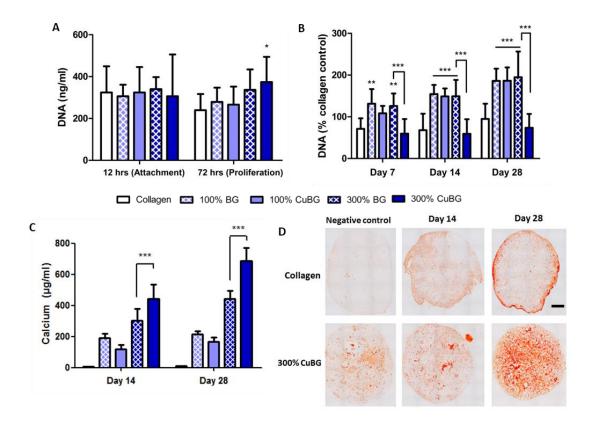


# Figure 6 Demonstration of the ability of copper-doped bioactive glass scaffolds to enhance osteogenesis

(A) PicoGreen<sup>®</sup> assay on scaffolds at 12 hours and 72 hours in growth medium as an indicator of initial cell attachment and proliferation, respectively. (B) PicoGreen<sup>®</sup> assay on scaffolds on days 7, 14, and 28 days after supplementation with osteogenic medium (DNA normalized to collagen control in growth media). (C) Total raw calcium values from scaffolds at day 14 and 28. (D) Alizarin red staining of scaffolds at day 14 and 28. Note: scale bar 1 mm. Data presented as mean  $\pm$  SD, n=3, p-values are calculated using two-way ANOVA with Bonferroni post-hoc test, all statistical significance shown in comparison to collagen control unless otherwise stated, \*p < 0.05, \*\*p < 0.01, \*\*\*p < 0.001.

#### 3.6 Copper-doped bioactive glass scaffolds enhance angiogenesis in vitro

Having determined that the CuBG-CS supports osteogenesis, we next investigated their ability to support angiogenesis, as copper has previously been suggested to be proangiogenic by upregulating VEGF production [16]. Note, while we did look at the effect of BG-CS controls – i.e. bioactive glass without copper-doping –as there was no significant difference to the collagen control, we have not included these results here. The eluate from CuBG-CS was shown to have a dose-dependent effect on VEGF protein production by MSCs (**Figure 7**A). At day 7 the 100% CuBG-CS significantly enhanced VEGF protein production, by 1.4 times vs. the collagen control (p < 0.01) while the 300% CuBG-CS performed similarly to the collagen control. The ability of the 100% CuBG-CS to enhance angiogenesis was further confirmed by observing the functional effect of increased VEGF production on total tubule length formed by HUVEC cells using a Matrigel<sup>®</sup> assay (**Figure 7**B). When tubule length was quantified, it was shown to be significantly enhanced for the 100% CuBG-CS group at day 1 (p < 0.001) by more than 1.9-fold in comparison to the collagen control (**Figure 7**C). This effect was not observed with the 300% CuBG-CS which showed significantly reduced tubule length at day 1, perhaps due to toxic effects on the sensitive HUVEC cells; however, by day 3 and 7, tubule length is recovered and the scaffolds perform similarly to the collagen control. Taking the Matrigel and VEGF protein production results together, this shows that CuBG scaffolds can enhance angiogenesis in a dose-dependent manner.

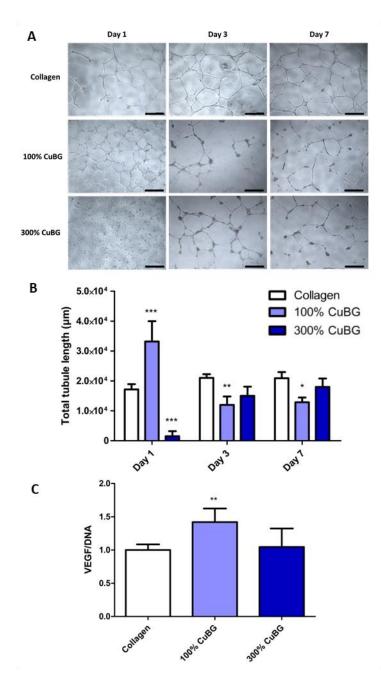


#### Figure 7 Effect of bioactive glass scaffolds on angiogenesis

(A) Brightfield images of tubule formation in Matrigel<sup>®</sup> assay at 36 hours post-seeding of human endothelial vascular endothelial (HUVEC) cells cultured with conditioned medium from collagen bioactive glass scaffolds. (B) Total tubule length ( $\mu$ m) quantification from Matrigel<sup>®</sup> assay. (C) VEGF protein production by rMSCs cultured with conditioned medium from collagen- bioactive glass scaffolds for 7 days (normalized to VEGF and DNA on collagen control). Note: scale bars 500  $\mu$ m. Data presented as mean ± SD, n=3, p-values are calculated using one- and two-way ANOVA with Bonferroni post-hoc test, all statistical significance shown in comparison to collagen control unless otherwise stated, \*p < 0.05, \*\*p < 0.01, \*\*\*p < 0.001.

# 3.7 Copper-doped bioactive glass scaffolds demonstrated enhanced osteo- and angiogenesis in a chick embryo ex ovo model

Having assessed the scaffolds comprehensively in a series of in vitro studies, we next sought to determine the effect of the different scaffold compositions on osteogenesis and angiogenesis in a more biologically complex chick embryo in vivo model. The hind limbs of the chicken embryos treated with BG-CS or CuBG-CS were harvested at day 12 of development and stained for alcian blue (for cartilage) and alizarin red (for bone). From visual inspection and quantification of the percentage of ossified limbs, similar to the in vitro studies, all bioactive glass treated scaffolds (both with and without copper doping) enhanced bone formation in comparison to collagen-only controls and to a similar level to the BMP-2 loaded control (**Figure 8** A&B).

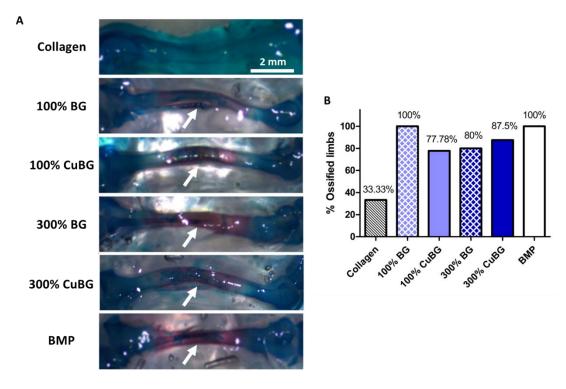


**Figure 8 Effect of bioactive glass scaffolds on osteogenesis in a chick embryo ex ovo model** (A) Representative images of chick embryo femora at day 12 of development stained with alcian blue and alizarin red after treatments with bioactive glass scaffolds or collagen only and BMP containing scaffolds as controls (10X magnification). Note: white arrows indicate alizarin red staining. (B) Quantified percentage of harvested limbs that stained positive for alizarin red, or mineralisation. Note: scale bar 2 mm.

In terms of angiogenesis, and again similar to the in vitro studies, 100% CuBG scaffolds show significantly enhanced angiogenesis in comparison to the collagen control both qualitatively and when quantified using image analysis software. Strikingly, these were more highly vascularised than the VEGF-loaded control (**Figure 9** A&B).

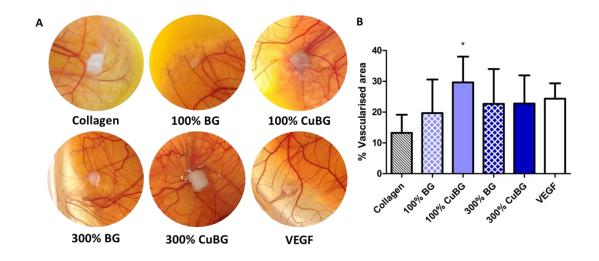


Figure 9 Effect of bioactive glass scaffolds on angiogenesis in a chick embryo ex ovo model (A) Representative images of the angiogenic response to bioactive glass scaffolds on the surrounding CAM membrane with collagen only and VEGF scaffolds as controls. (B) Quantified percentage vascularised area in a 12.5 mm Ø circular area around the scaffold treatments. Data presented as mean  $\pm$  SD, n=3, p-values are calculated using an unpaired two-tailed t-test with 95% CI, all statistical significance shown in comparison to collagen control unless otherwise stated, \*p < 0.05.

## 4. Discussion

The overall aim of this study was to investigate the effect of copper-doped bioactive glass (CuBG) incorporation into a porous collagen scaffold on the microarchitectural and mechanical properties, antibacterial activity, and the ability of the scaffolds to support osteogenesis and angiogenesis both in vitro and in vivo. The results demonstrate that these novel CuBG collagen scaffolds (CuBG-CS) were highly porous, had suitable pore size for successful bone tissue engineering, and showed increased compressive modulus in comparison to the BG-free collagen scaffold. Most importantly, CuBG addition was shown to result in antibacterial activity, demonstrating increased toxicity against S. aureus. Furthermore, in vitro, the incorporation of CuBG enhanced osteogenesis and angiogenesis in a dose-dependent manner. Most promisingly, when tested in a chick embryo ex ovo model, the CuBG-CS was not only biocompatible, showing no signs of toxicity, but also demonstrated the same pattern of enhanced osteo- and angiogenesis as the in vitro studies; indeed the CuBG-CS significantly outperformed VEGF positive controls in angiogenesis studies. Taken together, these results indicate that the CuBG-CS developed here show potential to be used in the osteomyelitis defect site by simultaneously limiting infection whilst promoting bone healing.

In this study, we proposed the development of a multi-functional scaffold for the treatment of bone defects and reduction of infection. This objective thus requires a matrix that is not only capable of supporting bone regeneration, but also inhibiting bacterial growth with the aim of avoiding contributing to antibiotic resistance. To the best of our knowledge, this is the first study to successfully demonstrate incorporation of copper-doped bioactive glass into a natural polymer-based scaffold. We found that the incorporation of CuBG into the collagen scaffold successfully resulted in a non-antibiotic antibacterial scaffold. The 300% CuBG-CS resulted in a significant reduction in *S. aureus* growth in comparison to the collagen control. Additionally, a time-kill assay showed that the 100% CuBG-CS and 300% CuBG-CS scaffolds also significantly delay the growth of *S. aureus* at 7 hours and from 7 to 24 hours, respectively, in comparison to the collagen control. There are a number of antibiotic-loaded collagen sponges (typically gentamicin) on the market for osteomyelitis treatment [54]; however, in clinical orthopaedic scenarios, these local antibiotic delivery vehicles are most often applied in a combined approach with the addition of systemic antibiotics to achieve the best possible results [55,56] Thus, from a clinical translation perspective, if the bacterial clearance and growth rate reduction we achieved here is not sufficient, a combined approach could be used.

As demonstrated in our 2-D studies – and consistent with many previous reports for both non-antibiotic antibacterials and antibiotics [57–61] – there is a fine balance between *S. aureus* toxicity and mammalian cell viability. However, in the 3D scaffold environment we found that in even at the highest CuBG concentration of 300%, mammalian cell number was not significantly reduced in comparison to the collagen control over the 28 days. Furthermore, with the exception of the 300% CuBG-CS, there is an increase in cell number on all scaffolds containing bioactive glass which may be partially attributed to the mechanical and microarchitectural properties of the BG-containing scaffolds; this would allow for more mechanically robust pores for cell attachment, infiltration, and proliferation.

We found that after trialling a number of different incorporation methods, that we can achieve a homogeneous distribution of bioactive glass throughout the collagen scaffold. The homogeneously distributed bioactive glass is advantageous as it would result in homogeneous mechanical properties, maximize surface area for contact with osteoprogenitor cells (and thus osteoconduction), and the increased surface area might also increase ion release and improve degradation [62,63]. Following addition of bioactive glass, all scaffolds remained over 98% porous. Previous work suggests porosities above 90% are necessary to ensure good cell infiltration and nutrient/waste transport throughout the construct; all scaffolds fabricated are in this range [64,65]. Additionally, the pore sizes in the developed CuBG-CS are within the ideal range for tissue engineering applications. Previous

studies have shown that pores of 40-100 µm show good cell viability and bone formation and pores within the 10-160 µm range are recommended for functional blood vessel formation [51–53]. Thus, we can surmise that the scaffold mean pore size range of 68-79 µm that we achieved is suitable for both osteogenesis and angiogenesis. Additionally, the scaffold compressive modulus was increased upon the addition of CuBG, with stiffness increased by 1.6-fold in 100% CuBG-CS and significantly by 2.7-fold in 300% CuBG scaffolds vs collagen alone. The incorporation of a ceramic into collagen-based scaffolds has been shown previously in our research group to increase stiffness [37,66]. This increase in stiffness is desirable for improved cell infiltration and proliferation and also for bone repair applications, as it has previously been shown that increased construct stiffness can influence the differentiation of mesenchymal stem cells (MSC) down an osteogenic lineage [67]. Additionally, the increase in compressive modulus we achieved is within the range of commercially available competitors and would also improve surgical handling due to the increased resistance to deformation, which would also maintain the critically important porosity and pore size [37].

It is widely described in the literature that bioactive glass is both osteoconductive and osteoinductive [17,68,69], additionally, it has also been shown that copper ions can promote osteogenesis [70,71]. This is consistent with our observations herein: significantly increased calcium deposition 300% CuBG-CS at day 14 and day 28 in comparison to the non-copper doped BG-CS and collagen only controls. Similarly, a previous in vivo study has shown that 3% (wt) copper-doped bioactive glass can enhance blood vessel formation and bone regeneration [72]. Another study demonstrated that the addition of 50  $\mu$ M of copper to MSCs diminished their proliferation rate and increased their ability to undergo osteogenic differentiation [15]. Thus, we can postulate that scaffold's enhanced bone regenerative capacity can be attributed to the combination of both the bioactive glass and copper within the CuBG-CS.

Many tissue engineered implants fail due to avascular necrosis [73–75]. Thus, effective vascularisation of porous scaffolds is a crucial event in successful tissue integration. There is an intimate relationship between vascularisation and improved bone formation, known as 'angiogenic–osteogenic coupling', so the invasion and development of a blood supply within the scaffold is essential for cell survival and flow of growth factors to stimulate the relationship [76–78]. In the current study, we see a dose-dependent response of endothelial cells to copper-doped bioactive glass scaffolds, with the lower dose 100% CuBG-CS significantly enhancing total tubule length by 1.9-fold. Copper ions have been shown

previously to have a pro-angiogenic effect on endothelial cells in vitro by upregulating VEGF production and enhancing proliferation [16,70,71,79,80]. In addition, it has been found that the combination of copper sulphate (50  $\mu$ g/ml – optimal dose) with the growth factors VEGF or FGF-2 on endothelial cells significantly enhanced the complexity of the angiogenic networks with a synergistic effect [81]. However, in our study, we also observed that the higher dose 300% CuBG-CS show significantly reduced tubule formation, which is presumed to be due to toxic effects on the cells. Another study reported a similar effect – 2.5% (mol) copper-doped Bioglass® decreased the ability of endothelial cells to form vascular networks with increasing CuBG addition and that, in fact, it is not due to increased copper release, but to increased silicon release and calcium depletion in the medium [82]. The authors also suggest that the proangiogenic effect of the copper released from the bioactive glass may not be reflected in endothelial cell cultures, but may upregulate angiogenic factors of fibroblasts or osteoblasts. Hence, we analysed VEGF protein production by rMSCs in 2D culture when cultured with conditioned medium from collagen bioactive glass scaffolds. The VEGF results demonstrated that the 100% CuBG scaffolds significantly increased VEGF protein production, which should contribute to enhanced angiogenesis; in addition, there was a direct effect on vessel formation in the Matrigel tubule assay. In any case, the obvious next step was to carry out an assessment of these novel materials in an in vivo study.

Having demonstrated the potential of the CuBG-CS in vitro, we next utilised an ex ovo (shellless) chicken embryo model to enable examination of the in vivo therapeutic effect of the scaffolds on angio- and osteogenesis [43–46]. The chick embryo ex ovo model is both economic and practical in comparison to other animal models as the fertilised eggs are plentiful and can be purchased year-round, they are low cost, they are housed in a regular lab-based incubator negating expensive specialist equipment and housing costs, the shellless model enables the continuous evaluation of the embryos. The experimental design involves culturing the chicken embryos for up to a maximum of 12 days which, although relatively short incubation period, can provide a plethora of results within a short time frame. Using this model, it was found that all of the bioactive-glass loaded scaffolds were biocompatible with no adverse reactions or reduction in survival of embryos observed. This is encouraging as it shows that the incorporation of the anti-microbial materials, while effective at eliminating bacteria, has no negative effect on adjacent healthy tissue. In fact the opposite effect was found and demonstrated enhanced osteogenesis and angiogenesis by the CuBG scaffolds in comparison to the collagen only controls – consistent with the in vitro study results. All bioactive glass-loaded scaffolds, with or without copper doping (100%

28

BG, 100% CuBG, 300% BG, and 300% CuBG), accelerated endochondral ossification in comparison to the collagen control and to similar levels to BMP-2-loaded positive control. These results correlate well with studies by Boccaccini et al. where 4555 Bioglass® scaffolds (4555 Bioglass®) also demonstrated enhanced osteogenesis in the chick embryo ex ovo model [46,83]. In terms of angiogenesis, again correlating with our in vitro findings, the 100% CuBG scaffolds significantly enhanced angiogenesis in comparison to the collagen control, and to a level higher than that of the VEGF-loaded positive control. To the best of our knowledge, this is the first report of copper-doped bioactive glass scaffolds analysed in the chicken embryo. We did not elicit an angiogenic response from either of the BG-CS (i.e. non copper-doped bioactive glass scaffolds), which is similar to results obtained by Vargas et al., Gorustovich et al., and Handel et al. who were also unable to detect an angiogenic response of un-doped 4555 Bioglass® on the chicken CAM membrane [46,83,84]. However, our results are also similar to a study by Durand et al., who saw a significant increase in angiogenesis on the CAM membrane when a therapeutic angiogenic metal ion, boron, was doped into 4555 Bioglass®, in comparison to non-boron doped Bioglass® [85].

The chick embryo model offers several economic and practical advantages over other in animal models and it provided valuable insight into the *in vivo* osteogenic and angiogenic effect of the scaffolds. However, it must be highlighted that the chick embryo model does not encompass an infection aspect, essential in assessing the suitability of potential new treatment strategies for osteomyelitis. Here, we used the chick embryo as a preliminary model to predict the response of the scaffolds within a complex biological environment before assessing the scaffolds in a full-scale osteomyelitis animal model. This strategy employed the 'three R's' principal, specifically 'replacement' and 'reduction' [86]. The animals within osteomyelitis models typically experience moderate-severe procedures, undergoing multiple surgeries over a long period of time. Thus, according to the first principal, substituting animals with alternatives which have a reduced capability of experiencing pain (such as the chick embryo here), encompasses replacement. Additionally, this intermediate animal model allowed us to select the lead-performing treatment groups before progressing to an osteomyelitis model, which refines the study resulting in a 'reduction' of animal numbers. Thus, having demonstrated efficacy through completing this intermediate animal study, in order to more comprehensively assess the antibacterial potential and regenerative capacity of these scaffolds, the obvious next step is to test these scaffolds in, for example, a rat or rabbit osteomyelitis model [87,88].

In summary, the copper-doped bioactive glass scaffolds developed here provide an environment that enhances both osteogenesis and angiogenesis when compared to collagen scaffolds alone and those with non-copper-doped bioactive glass. Of the groups examined, 100% CuBG and 300% CuBG scaffolds hold the most promise. Both scaffolds show significantly enhanced osteogenesis in vitro and in vivo. 100% CuBG-CS might be chosen for defects where there the infection risk is low and bone regeneration is a priority as it significantly enhanced tubule formation and VEGF protein production in vitro and angiogenesis in the chick embryo ex ovo model. Alternatively, the 300% CuBG-CS might be most suitable in a situation where an infection is present in the debridement site due to its enhanced antibacterial properties against S. aureus. Although 300% CuBG-CS showed some toxicity towards endothelial cells and inhibited their ability to form tubules, in an in vivo situation where the infection risk is high, the critical goal is to help the immune system clear the difficult-to-treat infection and there is a reservoir of new cells (e.g., in the marrow) that can replenish the scaffold once the initial burst of copper has been released i.e. we would expect limited cytotoxicity to endothelial cells in the clinical environment. This theory was further supported in our chick embryo ex ovo model where we did not detect any biocompatibility or toxicity issues.

### 5. Conclusion

Osteomyelitis is a notoriously difficult-to-treat infection that typically requires a two-stage treatment. Herein, we successfully produced a single-step approach to osteomyelitis treatment consisting of collagen copper-doped bioactive glass scaffolds capable of antibacterial activity, without the use of antibiotics, which also stimulate osteogenesis and angiogenesis both in vitro and in vivo. This platform system could be further modified and used to deliver a variety of other non-antibiotic antimicrobial metal ion-doped minerals. In summary, this study presents a single-stage, off-the-shelf treatment for osteomyelitis which might reduce the need for antibiotics and bone grafting thus reducing hospital stays and costs.

### Acknowledgements

The authors would like to acknowledge Brenton Cavanagh (RCSI) for developing an ImageJ script for Matrigel tubule length. ER would like to thank the Irish Research Council (GOIPG/2015/3044) for providing financial support to this study. For funding, CJK & FOB

acknowledge RCSI's Office of Research and Innovation Seed Fund Award (Grant no. GR 14–0963); Science Foundation Ireland (SFI) under Grant no. SFI/12/RC/2278 (the AMBER Centre), and the European Union for a Marie Curie European Reintegration Grant under H2020 (Project Reference 659715). CH and VN would like to acknowledge the following funding supports, SFI AMBER, SFI PIYRA, ERC StG 2D Nanocaps, ERC StG 2D Nanocaps, ERC CoG 3D2DPrint, Horizon2020 NMP Co-Pilot. CH And VN also thank the Advanced Microscopy Laboratory, Trinity College Dublin for provision of their facilities.

# **Disclosure of conflicts of interest**

The authors declare no competing financial interests.

# Data availability

The raw/processed data required to reproduce these findings cannot be shared at this time due to technical or time limitations.

## References

- G. Walter, M. Kemmerer, C. Kappler, R. Hoffmann, Treatment algorithms for chronic osteomyelitis, Dtsch. Arztebl. Int. 109 (2012) 257–264. doi:10.3238/arztebl.2012.0257.
- [2] A.L. Lima, P.R. Oliveira, V.C. Carvalho, S. Cimerman, E. Savio, Recommendations for the treatment of osteomyelitis, Brazilian J. Infect. Dis. 18 (2014) 526–534. doi:10.1016/j.bjid.2013.12.005.
- R. Kelsey, A. Kor, F. Cordano, Hematogenous osteomyelitis of the calcaneus in children: surgical treatment and use of implanted antibiotic beads., J. Foot Ankle Surg. 34 (1995) 547–555. doi:10.1016/S1067-2516(09)80076-8.
- J.H. Calhoun, M.M. Manring, M. Shirtliff, Osteomyelitis of the long bones, Semin. Plast. Surg. 23 (2009) 59–72. doi:10.1055/s-0029-1214158.
- [5] R.C. Fang, R.D. Galiano, Adjunctive therapies in the treatment of osteomyelitis, Semin. Plast. Surg. 23 (2009) 141–147. doi:10.1055/s-0029-1214166.
- [6] A.D. Tice, P.A. Hoaglund, D.A. Shoultz, Risk factors and treatment outcomes in osteomyelitis, (2003) 1261–1268. doi:10.1093/jac/dkg186.
- [7] R. Dimitriou, G.I. Mataliotakis, A.G. Angoules, N.K. Kanakaris, P. V Giannoudis, Complications following autologous bone graft harvesting from the iliac crest and using the RIA: A systematic review, Injury. 42 (2011) 3–15. doi:10.1016/j.injury.2011.06.015.
- [8] J.S. Gogia, J.P. Meehan, P.E. Di Cesare, A.A. Jamali, Local antibiotic therapy in osteomyelitis, Semin. Plast. Surg. 23 (2009) 100–107. doi:10.1055/s-0029-1214162.
- [9] Center for Drug Evaluation and Research, Information for Consumers (Drugs) Battle of the Bugs: Fighting Antibiotic Resistance, (2011). http://www.fda.gov/Drugs/ResourcesForYou/Consumers/ucm143568.htm

(accessed January 15, 2016).

- [10] CenterWatch, FDA approved drugs in infections and infectious diseases, (2017). http://www.centerwatch.com/drug-information/fda-approved-drugs/therapeuticarea/25/infections-and-infectious-diseases (accessed August 8, 2017).
- [11] C. Wu, Y. Zhou, M. Xu, P. Han, L. Chen, J. Chang, Y. Xiao, Copper-containing mesoporous bioactive glass scaffolds with multifunctional properties of angiogenesis capacity, osteostimulation and antibacterial activity, Biomaterials. 34 (2013) 422– 433. doi:10.1016/j.biomaterials.2012.09.066.
- Y.F. Goh, A.Z. Alshemary, M. Akram, M.R. Abdul Kadir, R. Hussain, Bioactive glass: an in-vitro comparative study of doping with nanoscale copper and silver particles, Int. J. Appl. Glas. Sci. 5 (2014) 255–266. doi:10.1111/jigg.12061.
- [13] D. Longano, N. Ditaranto, L. Sabbatini, L. Torsi, N. Cioffi, Synthesis and antimicrobial activity of copper nanomaterials, in: N. Cioffi, M. Rai (Eds.), Nano-Antimicrobials, Springer Berlin Heidelberg, 2011: pp. 85–117. doi:10.1007/978-3-642-24428-5\_3.
- [14] S.L.M. Dahl, R.B. Rucker, L.E. Niklason, Effects of copper and cross-linking on the extracellular matrix of tissue-engineered arteries, Cell Transplant. 14 (2005) 367–374. http://www.ncbi.nlm.nih.gov/pubmed/16180655.
- [15] J. Pablo Rodrguez, S. Ros, M. Gonzlez, Modulation of the proliferation and differentiation of human mesenchymal stem cells by copper, J. Cell. Biochem. 85 (2002) 92–100. doi:10.1002/jcb.10111.
- [16] S.N. Rath, A. Brandl, D. Hiller, A. Hoppe, U. Gbureck, R.E. Horch, A.R. Boccaccini, U. Kneser, Bioactive copper-doped glass scaffolds can stimulate endothelial cells in co-culture in combination with mesenchymal stem cells, PLoS One. 9 (2014) 1–24. doi:10.1371/journal.pone.0113319.
- [17] M.N. Rahaman, D.E. Day, B. Sonny Bal, Q. Fu, S.B. Jung, L.F. Bonewald, A.P. Tomsia, Bioactive glass in tissue engineering, Acta Biomater. 7 (2011) 2355–2373. doi:10.1016/j.actbio.2011.03.016.
- [18] F.G. Lyons, J.P. Gleeson, S. Partap, K. Coghlan, F.J. O'Brien, Novel microhydroxyapatite particles in a collagen scaffold: a bioactive bone void filler?, Clin. Orthop. Relat. Res. 472 (2014) 1318–1328. doi:10.1007/s11999-013-3438-0.
- [19] A.J. Ryan, F.J. O'Brien, Insoluble elastin reduces collagen scaffold stiffness, improves viscoelastic properties, and induces a contractile phenotype in smooth muscle cells, Biomaterials. 73 (2015) 296–307. doi:10.1016/j.biomaterials.2015.09.003.
- [20] P. Roche, T. Alekseeva, A. Widaa, A.J. Ryan, A. Matsiko, G. Duffy, F.J. O'Brien, M. Walsh, Olfactory neurospheres and peripheral nerve regeneration in a pre clinical model, Ir. J. Med. Sci. (2015) 116.
- [21] T.J. Levingstone, A. Ramesh, R.T. Brady, P.A.J. Brama, C. Kearney, J.P. Gleeson, F.J. O'Brien, Cell-free multi-layered collagen-based scaffolds demonstrate layer specific regeneration of functional osteochondral tissue in caprine joints, Biomaterials. 87 (2016) 69–81. doi:10.1016/j.biomaterials.2016.02.006.
- [22] C. O'Leary, B. Cavanagh, R.E. Unger, C.J. Kirkpatrick, S.O. Dea, F.J. O'Brien, S. Cryan, The development of a tissue-engineered tracheobronchial epithelial model using a bilayered collagen-hyaluronate scaffold, Biomaterials. 85 (2016) 111–127. doi:10.1016/j.biomaterials.2016.01.065.
- [23] F.J. O'Brien, Biomaterials & scaffolds for tissue engineering, Mater. Today. 14 (2011) 88–95. doi:10.1016/S1369-7021(11)70058-X.
- [24] G.M. Cunniffe, C.M. Curtin, E.M. Thompson, G.R. Dickson, F.J. O'Brien, Contentdependent osteogenic response of nanohydroxyapatite: an in vitro and in vivo assessment within collagen-based scaffolds, ACS Appl. Mater. Interfaces. 8 (2016) 23477–23488. doi:10.1021/acsami.6b06596.
- [25] L.L. Hench, R.J. Splinter, W.C. Allen, T.K. Greenlee, Bonding mechanisms at the

interface of ceramic prosthetic materials, J. Biomed. Mater. Res. 5 (1971) 117–141. doi:10.1002/jbm.820050611.

- [26] N. Lindfors, J. Geurts, P. Hyvonen, A. Suda, A. Domenico, S. Artiaco, C. Alizadeh, A. Brychcy, J. Bialecki, C. Romano, Antibacterial bioactive glass, S53P4, for chronic bone infections A multinational study, Adv. Exp. Med. Biol. 971 (2017) 81–92. doi:doi: 10.1007/5584\_2016\_156.
- [27] E. Quinlan, S. Partap, M.M. Azevedo, G. Jell, M.M. Stevens, F.J. O'Brien, Hypoxiamimicking bioactive glass/collagen glycosaminoglycan composite scaffolds to enhance angiogenesis and bone repair, Biomaterials. 52 (2015) 358–366. doi:10.1016/j.biomaterials.2015.02.006.
- [28] A. Oki, B. Parveen, S. Hossain, S. Adeniji, H. Donahue, Preparation and in vitro bioactivity of zinc containing sol-gel – derived bioglass materials, J. Biomed. Mater. Res. Part A. 69 (2004) 216–221. doi:10.1002/jbm.a.20070.
- [29] D. Kozon, K. Zheng, E. Boccardi, Y. Liu, L. Liverani, A.R. Boccaccini, Synthesis of monodispersed Ag-doped bioactive glass nanoparticles via surface modification, Materials (Basel). 9 (2016) 1–8. doi:10.3390/ma9040225.
- [30] F. Daivid, T.J. Levingstone, W. Schneeweiss, M. de Swarte, H. Jahns, J.P. Gleeson, F.J. O'Brien, Enhanced bone healing using collagen-hydroxyapatite scaffold implantation in the treatment of a large multiloculated mandibular aneurysmal bone cyst in a thoroughbred filly, J. Tissue Eng. Regen. Med. (2015) 1193–1199. doi:10.1002/term.
- [31] C. O'Leary, F.J. O'Brien, S.-A. Cryan, Retinoic acid-loaded collagen-hyaluronate scaffolds: a bioactive material for respiratory tissue regeneration, ACS Biomater. Sci. Eng. 3 (2017) 1381–1393. doi:10.1021/acsbiomaterials.6b00561.
- [32] R.M. Raftery, B. Woods, A.L.P. Marques, J. Moreira-Silva, T.H. Silva, S.A. Cryan, R.L. Reis, F.J. O'Brien, Multifunctional biomaterials from the sea: Assessing the effects of chitosan incorporation into collagen scaffolds on mechanical and biological functionality, Acta Biomater. 43 (2016) 160–169. doi:10.1016/j.actbio.2016.07.009.
- [33] F. Lebre, R. Sridharan, M.J. Sawkins, D.J. Kelly, F.J. O'Brien, E.C. Lavelle, The shape and size of hydroxyapatite particles dictate inflammatory responses following implantation, Sci. Rep. 7 (2017) 1–13. doi:10.1038/s41598-017-03086-0.
- [34] A.J. Ryan, J.P. Gleeson, A. Matsiko, E.M. Thompson, F.J. O'Brien, Effect of different hydroxyapatite incorporation methods on the structural and biological properties of porous collagen scaffolds for bone repair, J. Anat. 227 (2014) 732–745. doi:10.1111/joa.12262.
- [35] T.A. Scott, Refractive index of ethanol-water mixures and density and refractive index of ethanol-water-ethyl ether mixtures, J. Phys. Chem. 50 (1946) 406–412.
- [36] XL-SciTech, Bioactive Glass Microspheres: 4PiGraft(TM), (2013). http://xlscitech.com/products/Products-Functional.html (accessed July 24, 2017).
- [37] J.P. Gleeson, N.A. Plunkett, F.J. O'Brien, Addition of hydroxyapatite improves stiffness, interconnectivity and osteogenic potential of a highly porous collagenbased scaffold for bone tissue regeneration, Eur. Cells Mater. 20 (2010) 218–230.
- [38] F.J. O'Brien, B.A. Harley, I. V. Yannas, L. Gibson, Influence of freezing rate on pore structure in freeze-dried collagen-GAG scaffolds, Biomaterials. 25 (2004) 1077–1086. doi:10.1016/S0142-9612(03)00630-6.
- [39] M.G. Haugh, M.J. Jaasma, F.J. O'Brien, The effect of dehydrothermal treatment on the mechanical and structural properties of collagen-GAG scaffolds, J. Biomed. Mater. Res. - Part A. 89 (2009) 363–369. doi:10.1002/jbm.a.31955.
- [40] M.G. Haugh, C.M. Murphy, R.C. Mckiernan, C. Altenbuchner, F.J. O'Brien, Crosslinking and mechanical properties significantly influence cell attachment, proliferation, and migration within collagen glycosaminoglycan scaffolds, Tissue Eng. Part A. 17 (2011) 1201–1208.

- [41] P. Speulveda, J.R. Jones, L.L. Hench, Characterization of melt-derived 45S5 and solgel-derived 58S bioactive glasses, J. Biomed. Mater. Res. (2001) 564–569. doi:10.1002/jbm.0000.
- [42] I. V. Yannas, J.F. Burke, Design of an artificial skin. I. Basic design principles, J. Biomed. Mater. Res. 14 (1980) 65–81. doi:10.1002/jbm.820140108.
- [43] R.J. Wassersug, A procedure for differential staining of cartilage and bone in whole, formalin fixed vertebrates, Stain Technol. 51 (1976) 131–134. doi:10.3109/10520297609116684.
- [44] V. Hamburger, H.L. Hamilton, A series of normal stages in the development of the chick embryo, Dev. Dyn. 195 (1992) 231–272. doi:10.1002/aja.1001950404.
- [45] J. Luo, C. Redies, Ex ovo electroporation for gene transfer into older chicken embryos, Dev. Dyn. 233 (2005) 1470–1477. doi:10.1002/dvdy.20454.
- [46] G.E. Vargas, R.V. Mesones, O. Bretcanu, J.M.P. López, A.R. Boccaccini, A. Gorustovich, Biocompatibility and bone mineralization potential of 45S5 Bioglass<sup>®</sup>-derived glassceramic scaffolds in chick embryos, Acta Biomater. 5 (2009) 374–380. doi:10.1016/j.actbio.2008.07.016.
- [47] O. Elibol, J. Brake, Effect of egg turning angle and frequency during incubation on hatchability and incidence of unhatched broiler embryos with head in the small end of the egg, Poult. Sci. 85 (2006) 1433–1437. doi:10.1093/ps/85.8.1433.
- [48] R.J. Wasserbug, Wassersug76 a procedure for differential staining of cartilage and bone in whale formalin. fixed vertebrates.pdf.pdf, Stain Technol. 51 (1976) 131–133.
- [49] J. Bejarano, P. Caviedes, H. Palza, Sol gel synthesis and in vitro bioactivity of copper and zinc-doped silicate bioactive glasses and glass-ceramics, Biomed. Mater. 10 (2015) 1–13. doi:10.1088/1748-6041/10/2/025001.
- [50] J. Zeltinger, J.K. Sherwood, D.A. Graham, R. Müeller, L.G. Griffith, Effect of pore size and void fraction on cellular adhesion, proliferation, and matrix deposition, Tissue Eng. 7 (2001) 557–572. doi:10.1089/107632701753213183.
- [51] G. Akay, M.A. Birch, M.A. Bokhari, Microcellular polyHIPE polymer supports osteoblast growth and bone formation in vitro, Biomaterials. 25 (2004) 3991–4000. doi:10.1016/j.biomaterials.2003.10.086.
- [52] L.R. Madden, D.J. Mortisen, E.M. Sussman, S.K. Dupras, J.A. Fugate, J.L. Cuy, K.D. Hauch, M.A. Laflamme, C.E. Murry, B.D. Ratner, Proangiogenic scaffolds as functional templates for cardiac tissue engineering., Proc. Natl. Acad. Sci. U. S. A. 107 (2010) 15211–6. doi:10.1073/pnas.1006442107.
- [53] Q.L. Loh, C. Choong, Three-dimensional scaffolds for tissue engineering applications: role of porosity and pore size, Tissue Eng. Part B. Rev. 19 (2013) 485–502. doi:10.1089/ten.TEB.2012.0437.
- [54] N. Kavanagh, E.J. Ryan, A. Widaa, G. Sexton, J. Fennell, S. O'Rourk, K.C. Cahill, C.J. Kearney, F.J. O'Brien, S.W. Kerrigan, Staphylococcal osteomyelitis: Disease progression, treatment challenges, and future directions, Clin. Microbiol. Rev. 31 (2018) 1–25.
- [55] Tribute Pharmaceuticals Canada Inc., Collatamp G Orthopaedic Applications, (2018). https://collatampg.ca/Healthcare\_Professionals/Orthopaedic\_Applications/en (accessed February 15, 2018).
- [56] Biomet,SeptocollE,(2018).http://nl.biomet.be/viewversion.cfm?contentversionid=16834&sc=1(accessedFebruary 15, 2018).February 15, 2018).(accessed
- [57] N. Duewelhenke, O. Krut, P. Eysel, Influence on mitochondria and cytotoxicity of different antibiotics administered in high concentrations on primary human osteoblasts and cell lines, Antimicrob. Agents Chemother. 51 (2007) 54–63. doi:10.1128/AAC.00729-05.

- [58] P. Corneal, E. Cells, C. Chang, C. Lin, M. Tsai, Using MTT viability assay to test the cytotoxicity of antibiotics and steroid to cultured porcine corneal endothelial cells, J. Ocul. Pharmacol. 12 (1996).
- [59] M.B. Ferreira, S. Myiagi, C.G. Nogales, M.S. Campos, J.L. Lage-Marques, Time- and concentration-dependent cytotoxicity of antibiotics used in endodontic therapy., J. Appl. Oral Sci. 18 (2010) 259–63. doi:10.1590/S1678-77572010000300011.
- [60] O. Damour, S. Zhi Hua, F. Lasne, M. Villain, P. Rousselle, C. Collombel, Cytotoxicity evaluation of antiseptics and antibiotics on cultured human fibroblasts and keratinocytes, Burns. 18 (1992) 479–485. doi:10.1016/0305-4179(92)90180-3.
- [61] R.G. Contreras, J.R.S. Vilchis, H. Sakagami, Y. Nakamura, Y. Nakamura, Y. Hibino, H. Nakajima, J. Shimada, Type of cell death induced by seven metals in cultured mouse osteoblastic cells, In Vivo (Brooklyn). 24 (2010) 507–512. doi:24/4/507 [pii].
- [62] J. Chen, L. Zeng, X. Chen, T. Liao, J. Zheng, Preparation and characterization of bioactive glass tablets and evaluation of bioactivity and cytotoxicity in vitro, Bioact. Mater. 3 (2017) 315–321. doi:10.1016/j.bioactmat.2017.11.004.
- [63] D.M. Escobar-Sierra, J.S. Posada-Carvajal, D.L. Atehortúa-Soto, Fabrication of chitosan/bioactive glass composite scaffolds for medical applications, Rev. Tec. La Fac. Ing. Univ. Del Zulia. 40 (2017) 30–36. doi:10.17533/udea.redin.n80a05.
- [64] J.P. Gleeson, F.J. O'Brien, Composite scaffolds for orthopaedic regenerative medicine, Adv. Compos. Mater. Med. Nanotechnol. (2011) 33–58. http://cdn.intechweb.org/pdfs/14118.pdf.
- [65] K. Rezwan, Q.Z. Chen, J.J. Blaker, A. Roberto, Biodegradable and bioactive porous polymer / inorganic composite scaffolds for bone tissue engineering, 27 (2006) 3413– 3431. doi:10.1016/j.biomaterials.2006.01.039.
- [66] E. Quinlan, M. Azevedo, F.J. O'Brien, Hypoxia-mimicking bioactive glass / collagen glycosaminoglycan composite scaffolds to enhance angiogenesis and bone repair, Biomaterials. 52 (2015) 358–366. doi:10.1016/j.biomaterials.2015.02.006.
- [67] A.J. Engler, S. Sen, H.L. Sweeney, D.E. Discher, Matrix elasticity directs stem cell lineage specification, Cell. 126 (2006) 677–689. doi:10.1016/j.cell.2006.06.044.
- [68] L.-C. Gerhardt, A.R. Boccaccini, Bioactive glass and glass-ceramic scaffolds for bone tissue engineering, Materials (Basel). 3 (2010) 3867–3910. doi:10.3390/ma3073867.
- [69] L.L. Hench, Bioceramics, J. Am. Ceram. Soc. 81 (1998) 1705–1728. doi:10.1111/j.1151-2916.1998.tb02540.x.
- [70] H. Wang, S. Zhao, J. Zhou, Y. Shen, W. Huang, C. Zhang, M.N. Rahaman, D. Wang, Evaluation of borate bioactive glass scaffolds as a controlled delivery system for copper ions in stimulating osteogenesis and angiogenesis in bone healing, J. Mater. Chem. B. 2 (2014) 8547–8557. doi:10.1039/c4tb01355g.
- [71] Y. Lin, W. Xiao, B.S. Bal, M.N. Rahaman, Effect of copper-doped silicate 13-93 bioactive glass scaffolds on the response of MC3T3-E1 cells in vitro and on bone regeneration and angiogenesis in rat calvarial defects in vivo, Mater. Sci. Eng. C. 67 (2016) 440–452. doi:10.1016/j.msec.2016.05.073.
- [72] S. Zhao, H. Wang, Y. Zhang, W. Huang, M.N. Rahaman, Z. Liu, D. Wang, C. Zhang, Copper-doped borosilicate bioactive glass scaffolds with improved angiogenic and osteogenic capacity for repairing osseous defects., Acta Biomater. 14 (2015) 185–96. doi:10.1016/j.actbio.2014.12.010.
- [73] W.G. Chang, L.E. Niklason, A short discourse on vascular tissue engineering, Npj Regen. Med. 2 (2017) 1–7. doi:10.1038/s41536-017-0011-6.
- [74] E.C. Novosel, C. Kleinhans, P.J. Kluger, Vascularization is the key challenge in tissue engineering, Adv. Drug Deliv. Rev. 63 (2011) 300–311. doi:10.1016/j.addr.2011.03.004.
- [75] H.C.H. Ko, B.K. Milthorpe, C.D. McFarland, Engineering thick tissues The

vascularisation problem, Eur. Cells Mater. 14 (2007) 1–18. doi:10.22203/eCM.v014a01.

- [76] J. Barralet, U. Gbureck, P. Habibovic, E. Vorndran, C. Gerard, C.J. Doillon, Angiogenesis in Calcium Phosphate Scaffolds by Inorganic Copper Ion Release, Tissue Eng. Part A. 15 (2009) 1601–1609. doi:10.1089/ten.tea.2007.0370.
- [77] U.A. Gurkan, J. Gargac, O. Akkus, The sequential production profiles of growth factors and their relations to bone volume in ossifying bone marrow explants., Tissue Eng. Part A. 16 (2010) 2295–306. doi:10.1089/ten.TEA.2009.0565.
- [78] R.M. Raftery, I. Mencía Castaño, G. Chen, B. Cavanagh, B. Quinn, C.M. Curtin, S.A. Cryan, F.J. O'Brien, Translating the role of osteogenic-angiogenic coupling in bone formation: Highly efficient chitosan-pDNA activated scaffolds can accelerate bone regeneration in critical-sized bone defects, Biomaterials. 149 (2017) 116–127. doi:10.1016/j.biomaterials.2017.09.036.
- S. Li, H. Xie, S. Li, Y.J. Kang, Copper stimulates growth of human umbilical vein endothelial cells in a vascular endothelial growth factor-independent pathway, Exp. Biol. Med. (Maywood). 237 (2012) 77–82. doi:10.1258/ebm.2011.011267.
- [80] G.F. Hu, Copper stimulates proliferation of human endothelial cells under culture, J.
   Cell. Biochem. 69 (1998) 326–335. doi:10.1002/(SICI)1097-4644(19980601)69:3<326::AID-JCB10>3.0.CO;2-A.
- [81] C. Gérard, L.J. Bordeleau, J. Barralet, C.J. Doillon, The stimulation of angiogenesis and collagen deposition by copper, Biomaterials. 31 (2010) 824–831. doi:10.1016/j.biomaterials.2009.10.009.
- [82] C. Stähli, M. James-bhasin, A. Hoppe, A.R. Boccaccini, S.N. Nazhat, Effect of ion release from Cu-doped 45S5 Bioglass on 3D endothelial cell morphogenesis, 19 (2015) 15–22. doi:10.1016/j.actbio.2015.03.009.
- [83] A.A. Gorustovich, G.E. Vargas, O. Bretcanu, R. Vera Mesones, J.M. Porto López, A.R. Boccaccini, Novel bioassay to evaluate biocompatibility of bioactive glass scaffolds for tissue engineering, Adv. Appl. Ceram. 107 (2008) 274–276. doi:10.1179/174367508X306541.
- [84] M. Handel, T.R. Hammer, P. Nooeaid, A.R. Boccaccini, D. Hoefer, 45S5-Bioglass <sup>®</sup> based 3D-scaffolds seeded with human adipose tissue-derived stem cells induce in vivo vascularization in the CAM angiogenesis assay, Tissue Eng. Part A. 19 (2013) 2703–2712. doi:10.1089/ten.tea.2012.0707.
- [85] L.A. Haro Durand, G.E. Vargas, N.M. Romero, R. Vera-Mesones, J.M. Porto-López, A.R. Boccaccini, M.P. Zago, A. Baldi, A. Gorustovich, Angiogenic effects of ionic dissolution products released from a boron-doped 45S5 bioactive glass, J. Mater. Chem. B. 3 (2015) 1142–1148. doi:10.1039/c4tb01840k.
- [86] R. WMS, B. RL, The principles of humane experimental technique, Universities Federation for Animal Welfare, Wheathampstead (UK), 1959.
- [87] V.A. Stadelmann, I. Potapova, K. Camenisch, D. Nehrbass, R.G. Richards, T.F. Moriarty,
   Y. Chang, In vivo MicroCT monitoring of osteomyelitis in a rat model, Biomed Res. Int.
   2015 (2015). doi:10.1155/2015/587857.
- [88] D. Arens, M. Wilke, L. Calabro, S. Hackl, S. Zeiter, I. Zderic, R.G. Richards, T.F. Moriarty, A rabbit humerus model of plating and nailing osteosynthesis with and without Staphylococcus aureus osteomyelitis, Eur. Cells Mater. 30 (2015) 148–162. doi:10.22203/eCM.v030a11.